# Dynamic analysis of Kirchhoff-Love plates

## Classical structural elements

ME473 Dynamic finite element analysis of structures

Stefano Burzio

2025

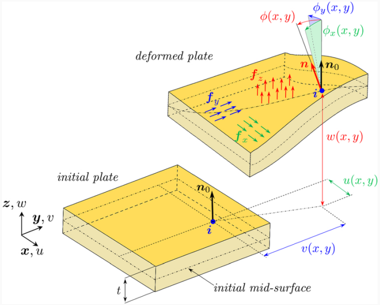

# Where do we stand?

| Week | Module | Lecture topic | Mini-projects |
|---|---|---|---|
| 1 | Linear elastodynamics | Strong and weak forms | |
| 2 | | Galerkin method | Groups formation |
| 3 | | FEM global | Project 1 statement |
| 4 | | FEM local | |
| 5 | | FEM local | Project 1 submission |
| 6 | Classical structural elements | Bars and trusses | Project 2 statement |
| 7 | | Beams | |
| 8 | | Frames and grids | |
| 9 | | Kirchhoff-Love plates | Project 2 submission |
| 10 | | Kirchhoff-Love plates | Project 3 statement |

## Summary

- Recap weeks 1-9
- AMC thin plate bending elements
- Example: modal analysis of a simply supported thin plate
- CR thin plate bending elements
- Example: modal analysis of a simply supported thin plate

## Recommended readings


(L) Logan, A first course in the finite element method, 6th ed. (chap. 12)

(P) Petyt, Introduction to finite element vibration analysis (chap. 6)

(O) Ochsner, PDE for classical structural members (chap. 7)

# Recap weeks 1-5: vibration of solids

# Statement of the linear elastodynamics problem

- **Object:**
  A solid $\Omega \subset \mathbb{R}^3$ with known material properties: $\mathbf{C}$ and $\rho$.
- **Main features:**
  - Acting loads on the body: $\mathbf{f}$.
  - Boundary $\Gamma = \Gamma_u \cup \Gamma_\sigma$ (the surface enclosing the solid).
  - Boundary conditions: prescribed displacements $\hat{\mathbf{u}}$ on $\Gamma_u$ and/or loads $\hat{\mathbf{f}}$ on $\Gamma_\sigma$.
  - Initial displacement $\mathbf{u}_0$ and velocity $\mathbf{v}_0$ at $t = 0$.

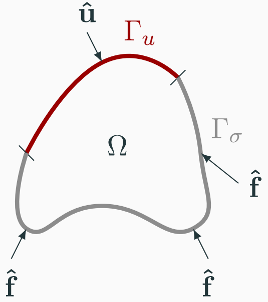

# Strong and semi-discrete weak forms of elastodynamics

## Strong form

PDE:
$$\nabla^T \mathbf{C} \nabla \mathbf{u} + \mathbf{f} = \rho \ddot{\mathbf{u}}$$

BC on $\Gamma_u$:
$$\mathbf{u} = \hat{\mathbf{u}}$$

BC on $\Gamma_\sigma$:
$$\mathbf{N}^T \mathbf{C} \nabla \mathbf{u} = \hat{\mathbf{f}}$$

IC at $t = 0$:
$$\mathbf{u} = \mathbf{u}_0, \ \dot{\mathbf{u}} = \mathbf{v}_0$$

## Semi-discrete weak form

ODE:
$$\delta \mathbf{q}^T \left[ \mathbf{M} \ddot{\mathbf{q}}(t) + \mathbf{K} \mathbf{q}(t) - \mathbf{r}(t) \right] = 0$$

Displacement approximation:
$$\mathbf{u}^h(\mathbf{x}, t) = \mathbf{H}(\mathbf{x}) \mathbf{q}(t) = \sum_{i=1}^{p} h_i(\mathbf{x}) \mathbf{q}_i(t)$$

IC at $t = 0$:
$$\mathbf{q}(0) = \mathbf{q_0}$$
$$\dot{\mathbf{q}}(0) = \mathbf{p_0}$$

# Displacements approximation in finte element method

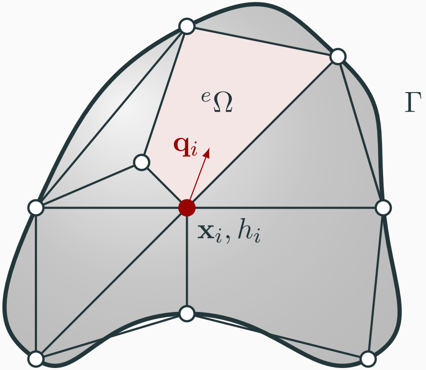


- **Stiffness matrix**:

$$\mathbf{K} = \int_\Omega \mathbf{B}^T \mathbf{C} \mathbf{B} \, d\Omega$$

where $\mathbf{B} = \nabla \mathbf{H}$.

- **Mass matrix**:

$$\mathbf{M} = \int_\Omega \rho \, \mathbf{H}^T \mathbf{H} \, d\Omega.$$

- **Applied forces vector**:

$$\mathbf{r}(t) = \int_{\Gamma_\sigma} \mathbf{H}^T \hat{\mathbf{f}} \, d\Gamma + \int_\Omega \mathbf{H}^T \mathbf{f} \, d\Omega.$$

# Recap weeks 6-8: vibration of 1d structures

**Truss**

- Structure composed of oriented bar (rod) elements, connected by frictionless pins, carrying **axial forces**.

**Frame**

- Structure composed of oriented beam elements, connected by welding, carrying **transversal, axial forces and torsion**.

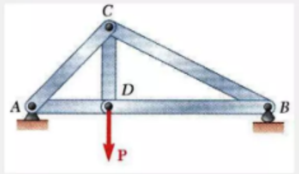


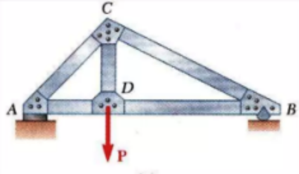

# Three-dimensional beam structure

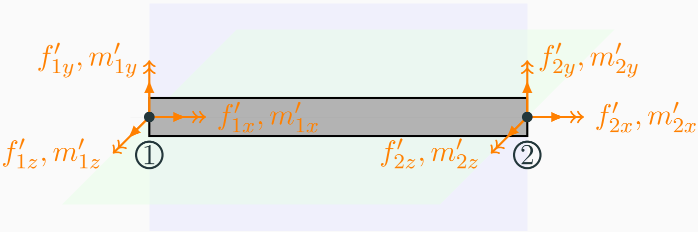


Three-dimensional beams are uniaxial (slender) element that can support:

- axial loads $f'_{ix}$,
- torsional loads $m'_{ix}$,
- bending in the $x' - y'$ plane: $f'_{iy}$ and $m'_{iz}$,
- bending in the $x' - z'$ plane: $f'_{iz}$ and $m'_{iy}$.

# Differential equations governing the dynamics

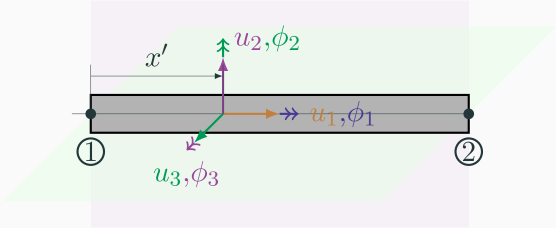


| | |
|---|---|
| *Bars* | $EA\partial^2_{x'x'}u_1(x',t) = \rho A\ddot{u}_1(x',t)$ |
| *Shafts* | $GJ\partial^2_{x'x'}\phi_1(x',t) = \rho J\ddot{\phi}_1(x',t)$ |
| *Planar beams* | $\partial^2_{x'x'}\left(EI_z\partial^2_{x'x'}u_2(x',t)\right) + \rho A\ddot{u}_2(x',t) = 0$ |
| *Planar beams* | $\partial^2_{x'x'}\left(EI_y\partial^2_{x'x'}u_3(x',t)\right) + \rho A\ddot{u}_3(x',t) = 0$ |

$I_y$ and $I_z$ are the cross-sectional moments of inertia with respect to the axes $y$ and $z$.

# Displacements discretization

Total of six nodal displacements at each unconstrained joint:

- three translation components $q'_{ix}$, $q'_{iy}$ and $q'_{iz}$ along the $x$, $y$, $z$ axes, and
- three rotational components about these axes $\phi'_{ix}$, $\phi'_{iy}$ and $\phi'_{iz}$.

$$u^h(x', t) = \mathbf{H}(x')\mathbf{q}_{loc}(t)$$

$$\mathbf{q}_{loc}(t) = \begin{bmatrix} q'_{1x}(t) \\ q'_{1y}(t) \\ q'_{1z}(t) \\ \phi'_{1x}(t) \\ \phi'_{1y}(t) \\ \phi'_{1z}(t) \\ q'_{2x}(t) \\ q'_{2y}(t) \\ q'_{2z}(t) \\ \phi'_{2x}(t) \\ \phi'_{2y}(t) \\ \phi'_{2z}(t) \end{bmatrix}$$

$$\begin{aligned}
h_1(x') &= 1 - x'/\ell & h_7(x') &= x'/\ell \\
h_2(x') &= 2(x'/\ell)^3 - 3(x'/\ell)^2 + 1 & h_8(x') &= 3(x'/\ell)^2 - 2(x'/\ell)^3 \\
h_3(x') &= 2(x'/\ell)^3 - 3(x'/\ell)^2 + 1 & h_9(x') &= 3(x'/\ell)^2 - 2(x'/\ell)^3 \\
h_4(x') &= 1 - x'/\ell & h_{10}(x') &= x'/\ell \\
h_5(x') &= x'(1 - x'/\ell)^2 & h_{11}(x') &= x'(x'/\ell)(x'/\ell - 1) \\
h_6(x') &= x'(1 - x'/\ell)^2 & h_{12}(x') &= x'(x'/\ell)(x'/\ell - 1)
\end{aligned}$$

# Recap week 9: vibration of 2d structures

# Plate structure

- Plate structures are geometrically similar to structures of the 2D plane stress problem, but it usually carries only **transversal loads** that lead to bending deformation of the plate.
- For example: floors of a building, aerospace and ships structures, etc...

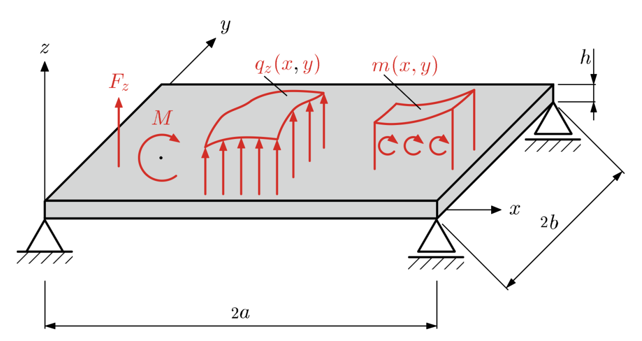


*(Credit: (O))*

# Kirchhoff assumption

**Rectilinearity and orthogonality of the cross-sectional normals**: Bernoulli's hypothesis is valid, i.e. a cross-sectional plane stays plane and perpendicular to the middle surface in the deformed state.

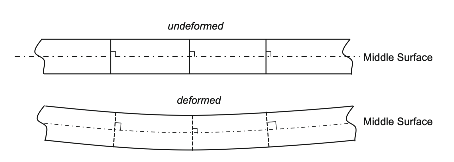


Shear strains $\varepsilon_{13}$ and $\varepsilon_{23}$ due to the distributed shear forces $q_x$ and $q_y$ are neglected.

*(Credit: (N))*

## Strong form for Kirchhoff-Love plate bending

Let $\Omega = [-a, a] \times [-b, b]$. Find the transverse displacement $u_3 \in C^4(\Omega \times [0, T])$ such that

$$\frac{h^3}{12} \boldsymbol{\nabla}_k^T \boldsymbol{C} \boldsymbol{\nabla}_k u_3 + \rho h \ddot{u}_3 = f_3 \qquad \text{on } \Omega \times ]0, T[ \tag{1}$$

boundary conditions (simply supported):

$$u_3 = 0 \qquad \text{in } \partial\Omega \times ]0, T[$$

$$\mathbf{M} = 0 \qquad \text{in } \partial\Omega \times ]0, T[$$

initial conditions:

$$u_3(\cdot, 0) = u_0 \quad \text{in } \Omega$$

$$\dot{u}_3(\cdot, 0) = v_0 \quad \text{in } \Omega$$

In case of isotropic material equation (1) reduces to

$$D \left( \frac{\partial^4 u_3}{\partial x_1^4} + 2 \frac{\partial^4 u_3}{\partial x_1^2 \partial x_2^2} + \frac{\partial^4 u_3}{\partial x_2^4} \right) + \rho h \ddot{u}_3 = f_3$$

where $D = Eh^3/(12(1-\nu^2))$.

# Weak form for Kirchhoff-Love plate bending

The weak form consists of finding the transverse displacement $u_3 \in \mathcal{U}$ such that the following equation is satisfied for every $\delta u_3 \in \mathcal{V}$:

$$\frac{h^3}{12} \int_\Omega \boldsymbol{\nabla}_k u_3 \mathbf{C}\, \boldsymbol{\nabla}_k \delta u_3 \, d\Omega + \int_\Omega \rho h \, \ddot{u}_3 \, \delta u_3 \, d\Omega = \int_\Omega f_3 \, \delta u_3 \, d\Omega$$

$$\mathcal{U} = \left\{ u_3(\cdot, t) \in H^2(\Omega) \mid u_3 = 0 \text{ in } \partial\Omega \times ]0, T[ \right\}$$

$$\mathcal{V} = \left\{ \delta u_3 \in H^2(\Omega) \mid \delta u_3 = 0 \text{ in } \partial\Omega \right\}$$

# Shell element

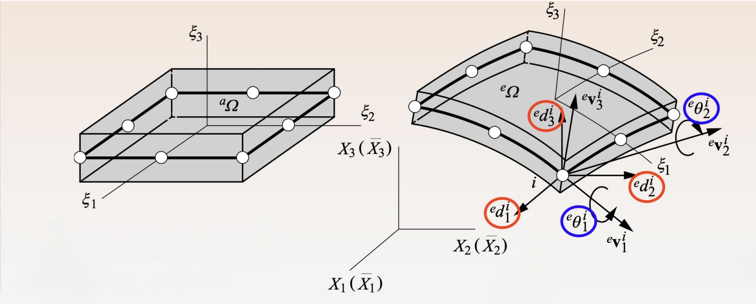


Shell elements:

- have 5 DOFs per node, no rotation $^e\theta_3^i$.
- lead to huge computational time savings since allow modeling with fewer mesh elements.
- less prone to negative Jacobian errors which might occur when using extremely thin 3d solid elements.

# Shape functions matrix

$$\mathbf{u}^h(\boldsymbol{\xi}) = \sum_{i=1}^{{}^e p} {}^a h_i(\xi_1, \xi_2) \left[ {}^e\mathbf{d}^i + \frac{1}{2}\xi_3 \, {}^e t_3^i \left( -{}^e\theta_1^i \, {}^e\mathbf{v}_2^i + {}^e\theta_2^i \, {}^e\mathbf{v}_1^i \right) \right]$$

$$= \sum_{i=1}^{{}^e p} {}^a\mathbf{H}_i(\boldsymbol{\xi}) \, {}^e\mathbf{q}^i(t)$$

$$= \sum_{i=1}^{{}^e p} \underbrace{\left[ \begin{array}{ccc|cc} {}^a h_i & 0 & 0 & -\frac{1}{2}\xi_3 \, {}^e t_3^i \, {}^a h_i \, {}^e v_{21}^i & \frac{1}{2}\xi_3 \, {}^e t_3^i \, {}^a h_i \, {}^e v_{11}^i \\ 0 & {}^a h_i & 0 & -\frac{1}{2}\xi_3 \, {}^e t_3^i \, {}^a h_i \, v_{22}^i & \frac{1}{2}\xi_3 \, {}^e t_3^i \, {}^a h_i \, {}^e v_{12}^i \\ 0 & 0 & {}^a h_i & -\frac{1}{2}\xi_3 \, {}^e t_3^i \, {}^a h_i \, {}^e v_{23}^i & \frac{1}{2}\xi_3 \, {}^e t_3^i \, {}^a h_i \, {}^e v_{13}^i \end{array} \right]}_{{}^a\mathbf{H}_i} \underbrace{\begin{bmatrix} {}^e d_1^i \\ {}^e d_2^i \\ {}^e d_3^i \\ {}^e \theta_1^i \\ {}^e \theta_2^i \end{bmatrix}}_{{}^e\mathbf{q}^i}$$

# Example: 8 nodes quadrangular shell element

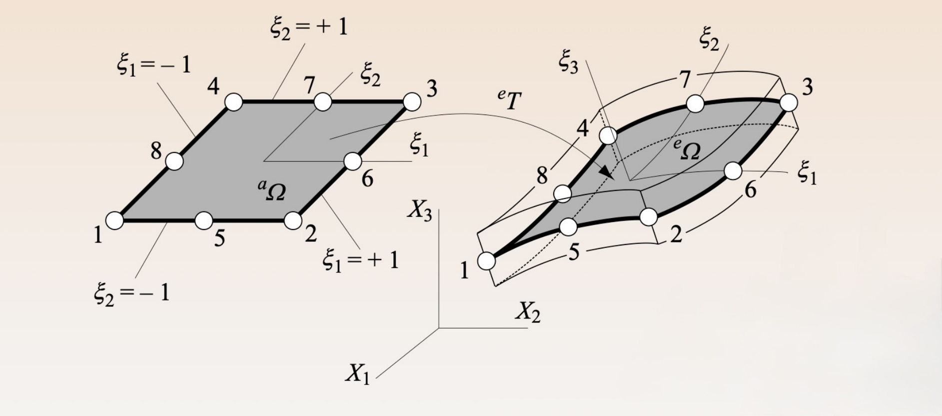

# Thin plate bending elements

# Overview of thin plate bending elements

Numerous finite elements for plate bending have been developed: **more than 88 distinct types** can be identified.

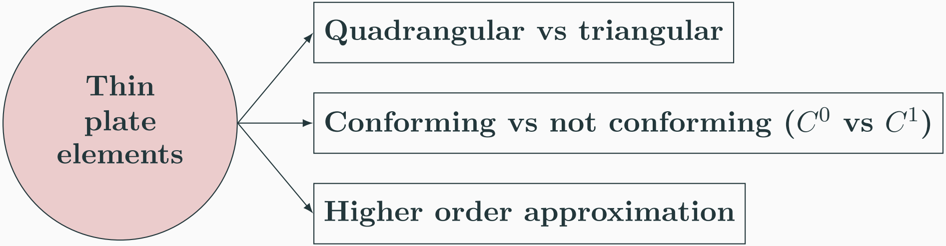


- **Adini-Melosh-Clough element (AMC)**: 12 dofs quadrangular, not conforming, thin plate.
- **Crouzeix–Raviart (CR)**: 16 dofs quadrangular, conforming, thin plate.

# Finite element approximation of Kirchhoff-Love plate

- Weak form equation

$$\frac{h^3}{12}\int_\Omega \boldsymbol{\nabla}_k u_3 \mathbf{C}\, \boldsymbol{\nabla}_k \delta u_3 \, d\Omega + \int_\Omega \rho h\, \ddot{u}_3 \, \delta u_3 \, d\Omega = \int_\Omega f_3 \, \delta u_3 \, d\Omega$$

- Semi-discrete weak form

$$\mathbf{M}\ddot{\mathbf{q}}(t) + \mathbf{K}\mathbf{q}(t) = \mathbf{r}(t)$$

Finite element approximation using polynomial shape functions:

$${}^e u_3^h(x_1, x_2, t) = \sum_{i=1}^{n} {}^e\mathbf{h}_i(x_1, x_2)\, {}^e\mathbf{q}^i(t) = {}^e\mathbf{H}(\mathbf{x})\, {}^e\mathbf{q}(t)$$

# Selection of the displacement function

To ensure convergence it is necessary to consider:

**Completeness criterion:**
highest order of derivatives in the weak form is 2.

→

Complete polynomials of at least degree 2:

$$
\begin{aligned}
{}^{e}u_3^h = & \, a_1 + a_2 x + a_3 y + \\
& + a_4 x^2 + a_5 xy + a_6 y^2 + \\
& + \text{higher order terms}
\end{aligned}
$$

**Continuity criterion:**
${}^{e}u_3^h$, $\partial_{x_1} {}^{e}u_3^h$, $\partial_{x_2} {}^{e}u_3^h$ are continuous between elements.

→

Each node $i$ has 3 DOFs:

- ${}^{e}d^i$ vertical displacement,
- ${}^{e}\theta_1^i$, ${}^{e}\theta_2^i$ rotations.

# AMC plate bending elements

# Selection of the displacement function

| | | | | | | | | | |
|---|---|---|---|---|---|---|---|---|---|
| | | | | $1$ | | | | | Constant |
| | | | $x_1$ | | $x_2$ | | | | Linear |
| | | $x_1^2$ | | $x_1 x_2$ | | $x_2^2$ | | | Quadratic |
| | $x_1^3$ | | $x_1^2 x_2$ | | $x_1 x_2^2$ | | $x_2^3$ | | Cubic |
| $x_1^4$ | | $x_1^3 x_2$ | | $x_1^2 x_2^2$ | | $x_1 x_2^3$ | | $x_2^4$ | Quartic |

**Displacement approximation** for rectangular elements with four nodes and thus 12 dofs: complete cubic polynomial, augmented with two (*geometrically invariant*) quartic terms

$$
\begin{aligned}
{}^{e}u_3^h(x_1, x_2, t) = {} & a_1 + a_2 x_1 + a_3 x_2 + a_4 x_1^2 + a_5 x_1 x_2 + a_6 x_2^2 + \\
& + a_7 x_1^3 + a_8 x_1^2 x_2 + a_9 x_1 x_2^2 + a_{10} x_2^3 + a_{11} x_1^3 x_2 + a_{12} x_1 x_2^3
\end{aligned}
$$

- ✓ Displacement approximation solves the unloaded strong form equation.
- ✓ Continuity in displacement along the interfaces of the elements.
- ✗ Slopes continuity along the interfaces are not ensured (*not conforming*).

The coordinate transformation:

$$ {}^eT : \Omega^a \to {}^e\Omega $$

$$ \boldsymbol{\xi} = \{\xi_1, \xi_2\}^T \mapsto \mathbf{x}(\boldsymbol{\xi}) = \{x_1(\boldsymbol{\xi}), x_2(\boldsymbol{\xi})\}^T = \{a\xi_1, b\xi_2\}^T $$

maps any point $\boldsymbol{\xi}$ in $\Omega^a = [-1, 1] \times [-1, 1]$ to its corresponding point of coordinate $\mathbf{x}(\boldsymbol{\xi})$ in ${}^e\Omega = [-a, a] \times [-b, b]$:

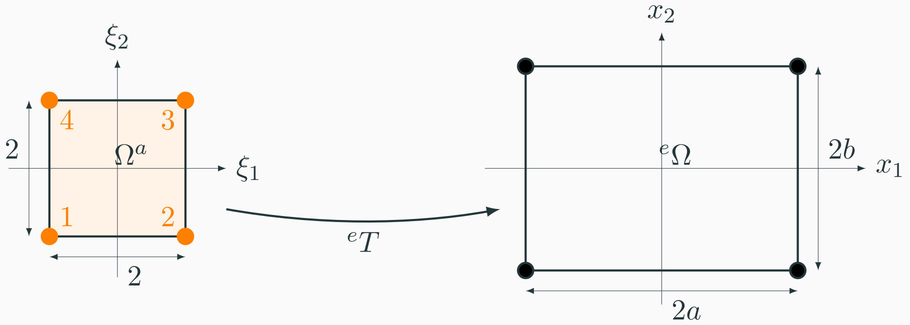

# Approximate displacement in local coordinates

$$^e u_3^h(\boldsymbol{\xi}, t) = \sum_{i=1}^{4} {}^a\mathbf{h}_i(\boldsymbol{\xi}) {}^e\mathbf{q}^i(t) = {}^a\mathbf{H}(\boldsymbol{\xi}) {}^e\mathbf{q}(t) = \begin{bmatrix} {}^a\mathbf{h}_1(\boldsymbol{\xi}) & {}^a\mathbf{h}_2(\boldsymbol{\xi}) & {}^a\mathbf{h}_3(\boldsymbol{\xi}) & {}^a\mathbf{h}_4(\boldsymbol{\xi}) \end{bmatrix} \begin{bmatrix} {}^e\mathbf{q}^1(t) \\ {}^e\mathbf{q}^2(t) \\ {}^e\mathbf{q}^3(t) \\ {}^e\mathbf{q}^4(t) \end{bmatrix}$$

where

- $^e\mathbf{q}^i(t) = \begin{bmatrix} {}^e d^i(t) \\ {}^e\theta_1^i(t) \\ {}^e\theta_2^i(t) \end{bmatrix} = \begin{bmatrix} {}^e u_3^h(\boldsymbol{\xi}^i, t) \\ \partial_{\xi_2} {}^e u_3^h(\boldsymbol{\xi}^i, t)/b \\ -\partial_{\xi_1} {}^e u_3^h(\boldsymbol{\xi}^i, t)/a \end{bmatrix}$
- $\boldsymbol{\xi}^i$ are the local coordinates of node $i$.

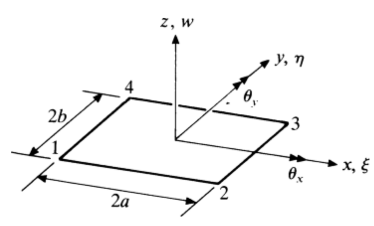

# Dofs in local coordinates

- Assumed form of the displacement function:

$$\begin{bmatrix} {}^e u_3^h \\ \partial_{\xi_2} {}^e u_3^h \\ \partial_{\xi_1} {}^e u_3^h \end{bmatrix} = \underbrace{\begin{bmatrix} 1 & \xi_1 & \xi_2 & \xi_1^2 & \xi_1\xi_2 & \xi_2^2 & \xi_1^3 & \xi_1^2\xi_2 & \xi_1\xi_2^2 & \xi_2^3 & \xi_1^3\xi_2 & \xi_1\xi_2^3 \\ 0 & 0 & 1 & 0 & \xi_1 & 2\xi_2 & 0 & \xi_1^2 & 2\xi_1\xi_2 & 3\xi_2^2 & \xi_1^3 & 3\xi_1\xi_2^2 \\ 0 & 1 & 0 & 2\xi_1 & \xi_2 & 0 & 3\xi_1^2 & 2\xi_1\xi_2 & \xi_2^2 & 0 & 3\xi_1^2\xi_2 & \xi_2^3 \end{bmatrix}}_{\mathbf{P}(\boldsymbol{\xi})} \underbrace{\begin{bmatrix} \alpha_1(t) \\ \vdots \\ \alpha_{12}(t) \end{bmatrix}}_{\boldsymbol{\alpha}(t)}$$

- Then the DOFs in local coordinates are:

$$ {}^e\mathbf{q}^i(t) = \underbrace{\begin{bmatrix} 1 & 0 & 0 \\ 0 & 1/b & 0 \\ 0 & 0 & -1/a \end{bmatrix} \mathbf{P}(\boldsymbol{\xi}^i)}_{\bar{\mathbf{P}}(\boldsymbol{\xi}^i)} \boldsymbol{\alpha}(t)$$

# Shape functions matrix for the AMC element

- Since

$$ {}^e\mathbf{q}(t) = \begin{bmatrix} {}^e\mathbf{q}^1(t) \\ {}^e\mathbf{q}^2(t) \\ {}^e\mathbf{q}^3(t) \\ {}^e\mathbf{q}^4(t) \end{bmatrix} = \underbrace{\begin{bmatrix} \bar{\mathbf{P}}(\boldsymbol{\xi}^1) \\ \bar{\mathbf{P}}(\boldsymbol{\xi}^2) \\ \bar{\mathbf{P}}(\boldsymbol{\xi}^3) \\ \bar{\mathbf{P}}(\boldsymbol{\xi}^4) \end{bmatrix}}_{\mathbf{A}} \boldsymbol{\alpha}(t) \qquad \Rightarrow \qquad \boldsymbol{\alpha}(t) = \mathbf{A}^{-1}\,{}^e\mathbf{q}(t) $$

- Then the shape functions matrix is ${}^a\mathbf{H} = \begin{bmatrix} {}^a\mathbf{h}_1 & {}^a\mathbf{h}_2 & {}^a\mathbf{h}_3 & {}^a\mathbf{h}_4 \end{bmatrix} = \mathbf{P}_1\mathbf{M}^{-1}$ where

$$ {}^a\mathbf{h}_i(\boldsymbol{\xi}) = \begin{bmatrix} (1+\xi_1^i\xi_1)(1+\xi_2^i\xi_2)(2+\xi_1^i\xi_1+\xi_2^i\xi_2-\xi_1^2-\xi_2^2)/8 \\ b(1+\xi_1^i\xi_1)(\xi_2^i+\xi_2)(\xi_2^2-1)/8 \\ -a(\xi_1^i+\xi_1)(\xi_1^2-1)(1+\xi_2^i\xi_2)/8 \end{bmatrix}^T $$

and $\boldsymbol{\xi}^i = \{\xi_1^i, \xi_2^i\}^T$ are the local coordinates of node $i$.

# Deformation, stiffness, mass matrices and loads vector

- ${}^a\mathbf{B} = \boldsymbol{\nabla}_k {}^a\mathbf{H}$ is a $(3 \times 12)$ matrix:

$$
{}^a\mathbf{B} = \begin{bmatrix} \frac{1}{a^2}\partial^2_{\xi_1} \\ \frac{1}{b^2}\partial^2_{\xi_2} \\ \frac{2}{ab}\partial^2_{\xi_1\xi_2} \end{bmatrix} \begin{bmatrix} {}^a\mathbf{h}_1 & {}^a\mathbf{h}_2 & {}^a\mathbf{h}_3 & {}^a\mathbf{h}_4 \end{bmatrix} = \begin{bmatrix} \begin{bmatrix} \frac{1}{a^2}\partial^2_{\xi_1} \\ \frac{1}{b^2}\partial^2_{\xi_2} \\ \frac{2}{ab}\partial^2_{\xi_1\xi_2} \end{bmatrix} {}^a\mathbf{h}_1 & \dots & \begin{bmatrix} \frac{1}{a^2}\partial^2_{\xi_1} \\ \frac{1}{b^2}\partial^2_{\xi_2} \\ \frac{2}{ab}\partial^2_{\xi_1\xi_2} \end{bmatrix} {}^a\mathbf{h}_4 \end{bmatrix}
$$

- ${}^e\mathbf{K}$ and ${}^e\mathbf{M}$ are $(12 \times 12)$ matrices and ${}^e\mathbf{r}$ is a $(12 \times 1)$ vector:

$$
{}^e\mathbf{K} = \frac{h^3}{12} \int_\Omega {}^e\mathbf{B}^T \mathbf{C} {}^e\mathbf{B} \, d\Omega = \frac{h^3 ab}{12} \int_{-1}^1 \int_{-1}^1 {}^a\mathbf{B}^T \mathbf{C} {}^a\mathbf{B} \, d\xi_1 d\xi_2,
$$

$$
{}^e\mathbf{M} = \int_\Omega \rho h \, {}^e\mathbf{H}^T {}^e\mathbf{H} \, d\Omega = \rho h ab \int_{-1}^1 \int_{-1}^1 {}^a\mathbf{H}^T {}^a\mathbf{H} \, d\xi_1 d\xi_2,
$$

$$
\mathbf{r}(t) = \int_\Omega \mathbf{H}^T f_3(t) \, d\Omega = ab f_3(t) \int_{-1}^1 \int_{-1}^1 {}^a\mathbf{H}^T \, d\xi_1 d\xi_2.
$$

# Post processing

- The approximated stresses at any point $(x_1, x_2, x_3)$ of the element $e$ are given in term of the nodal displacements:

$$^{e}\boldsymbol{\sigma}^{h} = \mathbf{C}^{e}\boldsymbol{\varepsilon}^{h} = -x_3\mathbf{C}\boldsymbol{\nabla}_{k}{}^{e}u_3^h = -x_3\mathbf{C}^{e}\mathbf{B}^{e}\mathbf{q}(t)$$

- The approximated bending moments $M_{11}^h$ and $M_{22}^h$ and twisting moment $M_{12}^h$ per unit length are given by:

$$\mathbf{M} = \begin{bmatrix} M_{11}^h \\ M_{22}^h \\ M_{12}^h \end{bmatrix} = \int_{-\frac{h}{2}}^{\frac{h}{2}} x_3 \begin{bmatrix} \sigma_{11}^h \\ \sigma_{22}^h \\ \sigma_{12}^h \end{bmatrix} dx_3 = -\frac{h^3}{12}\boldsymbol{C}^{e}\mathbf{B}^{e}\mathbf{q}(t)$$

# Example: isotropic square plate in free vibrations

Use the ACM element to estimate the five lowest frequencies of a square plate ($\ell \times \ell$) which is simply supported on all four edges.

Compare the results with the analytical solution

$$\omega_{m,n} = \pi^2 \frac{m^2 + n^2}{\ell^2} \sqrt{\frac{D}{\rho h}} \text{ rad/s},$$

where $\ell$ is the length of each side and $(m, n)$ are the number of half-waves in the $x$- and $y$-directions and $D$ is flexural rigidity of the plate:

$$D = \frac{Eh^3}{12(1 - \nu^2)}.$$

# Boundary conditions

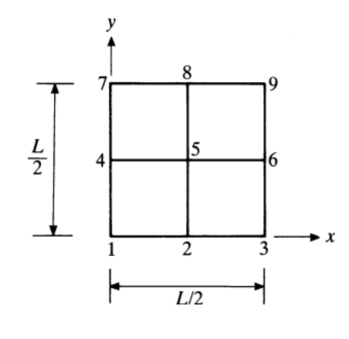


**Figure 1:** One-quarter of the plate represented by four rectangular elements.

*(Credit: (P))*

- **Simple support**:
  - sides 1-3: $u_3 = \theta_2 = 0$ at nodes 1, 2, and 3,
  - sides 1-7: $u_3 = \theta_1 = 0$ at nodes 1, 4, and 7.
- **Symmetric modes**:
  - with respect to side 3-9: $\theta_2 = 0$ at nodes 3, 6, and 9,
  - with respect to side 7-9: $\theta_1 = 0$ at nodes 7, 8, and 9.
- **Antisymmetric modes**:
  - with respect to side 3-9: $u_3 = \theta_1 = 0$ at nodes 3, 6, and 9.
  - with respect to side 7-9: $u_3 = \theta_2 = 0$ at nodes 7, 8, and 9.

# Frequencies estimate for square plate with ACM element

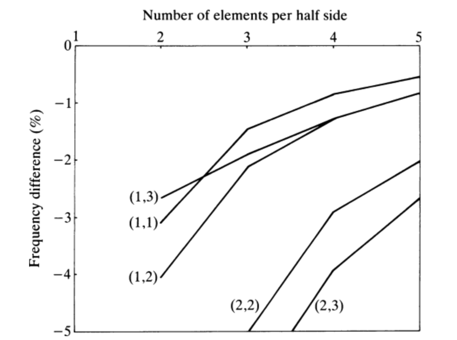


**Figure 2:** Relative errors for simply supported (S) square plate.

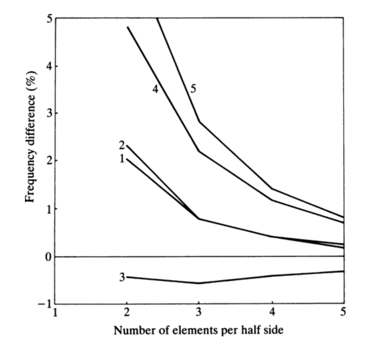


**Figure 3:** Relative errors for simply supported (S)/free (F) square plate.

*(Credit: (P))*

# Modal patterns

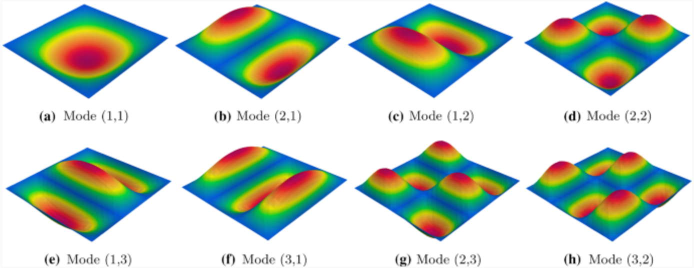


**Figure 4:** Vibration mode shape for a simply supported (S) square plate.

*(Credit: Pagani, Azzara, Carrera - Geometrically nonlinear analysis and vibration of in-plane-loaded variable angle tow composite plates and shells)*

# Modal patterns

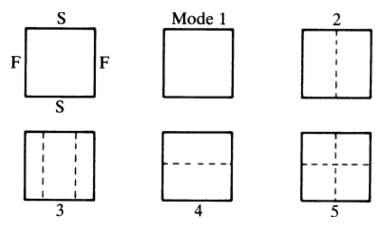


**Figure 5:** Mode shapes of a simply supported (S)/free (F) square plate.

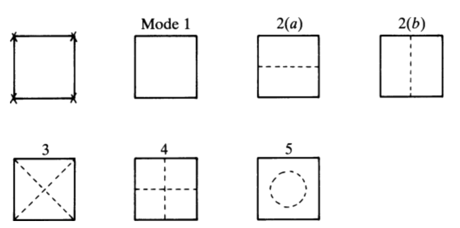


**Figure 6:** Mode shapes of a corner supported square plate.

*(Credit: (P))*

# Frequencies estimate for square plate with AMC element

First six natural frequencies of a square plate of side $\ell = 0.3048$ m and thickness $h = 3.2766$ mm which is point supported at its four corners.
$E = 73.084 \cdot 10^9$ N/m$^2$, $\nu = 0.3$, $\rho = 2821$ kg/m$^3$.

| | FEM [6.9] | | Analytical | | Experimental |
|---|---|---|---|---|---|
| Mode | $(2 \times 2)$ | $(4 \times 4)$ | [6.7] | [6.8] | [6.7] |
| 1 | 62.15 | 62.09 | 61.4 | 61.11 | 62 |
| 2$(a)$, $(b)$ | 141.0 | 138.5 | 136 | 134.6 | 134 |
| 3 | 169.7 | 169.7 | 170 | 166.3 | 169 |
| 4 | 343.7 | 340.0 | 333 | 331.9 | 330 |
| 5 | 397.4 | 396.0 | 385 | 383.1 | 383 |

**Figure 7:** Comparison of predicted and analytical frequencies of a corner supported square plate

# CR thin plate bending elements

# Selection of the displacement function

| Terms | Degree |
|---|---|
| $1$ | Constant |
| $x_1 \quad x_2$ | Linear |
| $x_1^2 \quad x_1 x_2 \quad x_2^2$ | Quadratic |
| $x_1^3 \quad x_1^2 x_2 \quad x_1 x_2^2 \quad x_2^3$ | Cubic |
| $x_1^3 x_2 \quad x_1^2 x_2^2 \quad x_1 x_2^3$ | Quartic |
| $x_1^3 x_2^2 \quad x_1^2 x_2^3$ | Quintic |
| $x_1^3 x_2^3$ | Sextic |

**Displacement approximation** for rectangular elements with four nodes and 16 dofs (4 dofs per node): complete cubic polynomial, augmented with three quartic, two quintic and one sextic terms:

$$\begin{aligned} {}^e u_3^h(x_1, x_2, t) = & \, a_1 + a_2 x_1 + a_3 x_2 + a_4 x_1^2 + a_5 x_1 x_2 + a_6 x_2^2 + \\ & + a_7 x_1^3 + a_8 x_1^2 x_2 + a_9 x_1 x_2^2 + a_{10} x_2^3 + \\ & + a_{11} x_1^3 x_2 + a_{12} x_1 x_2^3 + a_{13} x^2 y^2 + a_{14} x^3 y^2 + a_{15} x^2 y^3 + a_{16} x^3 y^3 \end{aligned}$$

# Recall: transversal bending for Euler-Bernoulli beam

Approximated transversal displacement $u_2^h$ as a function of the nodal DOFs:

$$^e u_2^h(\xi, t) = \mathbf{H}(\xi)\mathbf{q}(t) = [h_1(\xi),\ h_2(\xi),\ h_3(\xi),\ h_4(\xi)] \begin{bmatrix} d^1(t) \\ \theta^1(t) \\ d^2(t) \\ \theta^2(t) \end{bmatrix}$$

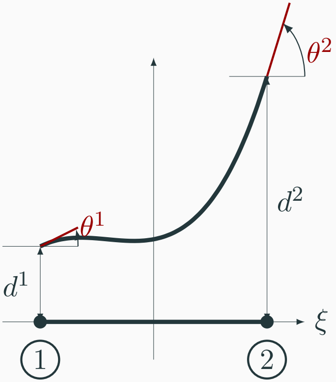


**$C^1$ Hermite shape functions on $[-1, 1]$:**

$$h_1(\xi) = (\xi^3 - 3\xi + 2)/4$$
$$h_3(\xi) = (-\xi^3 + 3\xi + 2)/4$$
$$h_2(\xi) = (\xi^3 - \xi^2 - \xi + 1)/4$$
$$h_4(\xi) = (\xi^3 + \xi^2 - \xi - 1)/4$$

## Shape functions matrix: a first try

- Let $\xi^i$ be the coordinate of the node $i$. Then the Hermite shape functions matrix is $\mathbf{H}(\xi) = [f_1 \; g_1 \; f_2 \; g_2]$ where

$$f_i(\xi) = (-\xi^i \xi^3 + 3\xi^i \xi + 2)/4 \qquad g_i(\xi) = (\xi^3 + \xi^i \xi^2 - \xi - \xi^i)/4.$$

- The shape functions matrix for the plate bending element is a product of Hermite functions:

$$^a\mathbf{H} = \begin{bmatrix} ^a\mathbf{h}_1 & ^a\mathbf{h}_2 & ^a\mathbf{h}_3 & ^a\mathbf{h}_4 \end{bmatrix}$$

where

$$^a\mathbf{h}_i(\boldsymbol{\xi}) = \begin{bmatrix} f_i(\xi_1) f_i(\xi_2) \\ b f_i(\xi_1) g_i(\xi_2) \\ -a g_i(\xi_1) f_i(\xi_2) \end{bmatrix}^T .$$

# Zero-twist constraint

- The approximate displacement in local coordinate is defined as:

$$ {}^{e}u_3^h(\boldsymbol{\xi},t) = \sum_{i=1}^{4} {}^{a}\mathbf{h}_i(\xi_1,\xi_2)\,{}^{e}\mathbf{q}^i(t) = {}^{a}\mathbf{H}(\boldsymbol{\xi})\,{}^{e}\mathbf{q}(t) $$

✗ The twist

$$ \frac{\partial^2}{\partial\xi_1\partial\xi_2}\,{}^{e}u_3^h(\boldsymbol{\xi},t) $$

is zero at the four nodal points. Thus the plate will tend to a zero twist condition as an increasing number of elements are used.

**Solution:** introduce

$$ \theta_{12}^i = \frac{\partial^2}{\partial\xi_1\partial\xi_2}\,{}^{e}u_3^h(\boldsymbol{\xi}^i,t) $$

as an extra degree of freedom.

# Shape functions matrix for the CR element

The approximate displacement in local coordinate is defined as:

$$ {}^{e}u_3^h(\boldsymbol{\xi}, t) = \sum_{i=1}^{4} {}^{a}\mathbf{h}_i(\boldsymbol{\xi}) {}^{e}\mathbf{q}^i(t) = {}^{a}\mathbf{H}(\boldsymbol{\xi}) {}^{e}\mathbf{q}(t) $$

- 4 dofs per node: $ {}^{e}\mathbf{q}^i(t) = \begin{bmatrix} {}^{e}d^i(t) \\ {}^{e}\theta_1^i(t) \\ {}^{e}\theta_2^i(t) \\ {}^{e}\theta_{12}^i(t) \end{bmatrix} = \begin{bmatrix} {}^{e}u_3^h(\boldsymbol{\xi}^i, t) \\ \partial_{\xi_2} {}^{e}u_3^h(\boldsymbol{\xi}^i, t)/b \\ -\partial_{\xi_1} {}^{e}u_3^h(\boldsymbol{\xi}^i, t)/a \\ \partial^2_{\xi_1\xi_2} {}^{e}u_3^h(\boldsymbol{\xi}^i, t)/(ab) \end{bmatrix} $
- The shape function matrix is ${}^{a}\mathbf{H} = \begin{bmatrix} {}^{a}\mathbf{h}_1 & {}^{a}\mathbf{h}_2 & {}^{a}\mathbf{h}_3 & {}^{a}\mathbf{h}_4 \end{bmatrix}$ where

$$ {}^{a}\mathbf{h}_i(\boldsymbol{\xi}) = \begin{bmatrix} f_i(\xi_1) f_i(\xi_2) \\ b f_i(\xi_1) g_i(\xi_2) \\ -a g_i(\xi_1) f_i(\xi_2) \\ ab g_i(\xi_1) g_i(\xi_2) \end{bmatrix}^T $$

# Boundary conditions

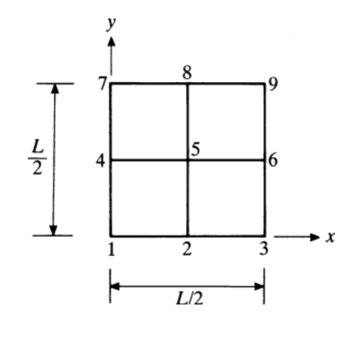


**Figure 8:** One-quarter of the plate represented by four rectangular elements.

*(Credit: (P))*

- **Simple support**:
  - sides 1-3: $u_3 = \theta_2 = 0$ at nodes 1, 2, and 3,
  - sides 1-7: $u_3 = \theta_1 = 0$ at nodes 1, 4, and 7.
- **Symmetric modes**:
  - with respect to side 3-9: $\theta_2 = \theta_{12} = 0$ at nodes 3, 6, and 9,
  - with respect to side 7-9: $\theta_1 = \theta_{12} = 0$ at nodes 7, 8, and 9.
- **Antisymmetric modes**:
  - with respect to side 3-9: $u_3 = \theta_1 = 0$ at nodes 3, 6, and 9.
  - with respect to side 7-9: $u_3 = \theta_2 = 0$ at nodes 7, 8, and 9.

# Example: isotropic square plate in free vibrations

# Frequencies estimate for square plate with CR element

The CR element is used to estimate the first lowest frequencies of a square plate $(\ell \times \ell)$ which is simply supported on all four edges.

| | FEM grids ($\frac{1}{4}$ plate) | | | |
|---|---|---|---|---|
| Mode | $2 \times 2$ | $3 \times 3$ | $4 \times 4$ | $5 \times 5$ |
| (1, 1) | 0.02 | 0.01 | 0.0 | 0.0 |
| (1, 2), (2, 1) | 0.26 | 0.05 | 0.02 | 0.01 |
| (2, 2) | 0.22 | 0.04 | 0.01 | 0.01 |
| (1, 3), (3, 1) | 1.51 | 0.32 | 0.11 | 0.04 |
| (2, 3), (3, 2) | 0.99 | 0.21 | 0.07 | 0.03 |

**Figure 9:** Relative errors for simply supported (S) square plate.

# Frequencies estimate for square plate with CR element

First six natural frequencies of a square plate of side $\ell = 0.3048$ m and thickness $h = 3.2766$ mm which is point supported at its four corners.
$E = 73.084 \cdot 10^9$ N/m$^2$, $\nu = 0.3$, $\rho = 2821$ kg/m$^3$.

| | FEM [6.9] (CR) | | Analytical | | Experimental |
|---|---|---|---|---|---|
| Mode | $(2 \times 2)$ | $(4 \times 4)$ | [6.7] | [6.8] | [6.7] |
| 1 | 62.03 | 61.79 | 61.4 | 62.11 | 62 |
| 2(*a*), (*b*) | 138.9 | 134.9 | 136 | 134.6 | 134 |
| 3 | 169.7 | 169.6 | 170 | 166.3 | 169 |
| 4 | 338.9 | 335.1 | 333 | 331.9 | 330 |
| 5 | 391.5 | 387.5 | 385 | 383.1 | 383 |

**Figure 10:** Comparison of predicted and analytical frequencies of a corner supported square plate

# Comparison: AMC vs CR plate bending element

**CR element (Conforming)**

- 4 degrees of freedom per node: $u_3$, $\theta_1$, $\theta_2$, and $\theta_{12}$.
- Displacement $u_3$ and rotations $\theta_1, \theta_2$ are continuous across element boundaries.
- Fully conforming to the $C^1$ continuity required by Kirchhoff plate theory.
- Higher computational cost and complexity.

**AMC element (Nonconforming)**

- 3 degrees of freedom per node: $u_3$, $\theta_1$, $\theta_2$.
- Only displacement $u_3$ is continuous across elements; rotations may have jumps.
- Nonconforming element: does not fully satisfy $C^1$ continuity.
- Simpler and computationally cheaper; suitable for practical applications.

# Why would you use AMC element if it's nonconforming?

- Computationally cheaper than full $C^1$ elements (fewer dofs).
- It still converges (theoretical results for nonconforming FEMs show convergence under certain conditions).
- Suitable when small slope discontinuities are acceptable (e.g., dynamic problems, large meshes).
- Tends to underestimate the natural frequencies, making it a useful benchmark for detecting overstiffness in numerical model.